Am. J. Hum. Genet. 67:814–821, 2000

A Novel Nemaline Myopathy in the Amish Caused by a Mutation in Troponin T1

Jennifer J. Johnston,[1] Richard I. Kelley,[5,7] Thomas O. Crawford,[6] D. Holmes Morton,[7] Richa Agarwala,[3] Thorsten Koch,[8] Alejandro A. Schäffer,[4] Clair A. Francomano,[1] and Leslie G. Biesecker[2]

[1]Medical Genetics Branch and [2]Genetic Disease Research Branch, National Human Genome Research Institute, [3]Information Engineering Branch, and [4]Computational Biology Branch, National Center for Biotechnology Information, National Institutes of Health, Bethesda; [5]Kennedy Krieger Institute and Department of Pediatrics and [6]Department of Neurology and Pediatrics, Johns Hopkins University, Baltimore; [7]The Clinic for Special Children, Strasburg, PA; and [8]Konrad-Zuse-Zentrum für Informationstechnik, Berlin

The nemaline myopathies are characterized by weakness and eosinophilic, rodlike (nemaline) inclusions in muscle fibers. Amish nemaline myopathy is a form of nemaline myopathy common among the Old Order Amish. In the first months of life, affected infants have tremors with hypotonia and mild contractures of the shoulders and hips. Progressive worsening of the proximal contractures, weakness, and a pectus carinatum deformity develop before the children die of respiratory insufficiency, usually in the second year. The disorder has an incidence of ~1 in 500 among the Amish, and it is inherited in an autosomal recessive pattern. Using a genealogy database, automated pedigree software, and linkage analysis of DNA samples from four sibships, we identified an ~2-cM interval on chromosome 19q13.4 that was homozygous in all affected individuals. The gene for the sarcomeric thin-filament protein, slow skeletal muscle troponin T (*TNNT1*), maps to this interval and was sequenced. We identified a stop codon in exon 11, predicted to truncate the protein at amino acid 179, which segregates with the disease. We conclude that Amish nemaline myopathy is a distinct, heritable, myopathic disorder caused by a mutation in *TNNT1*.

Introduction

The nemaline myopathies (NM [MIM 256030, 161800]) are neuromuscular disorders characterized by muscle weakness and rod-shaped "nemaline" inclusions in skeletal muscle fibers (North et al. 1997). NM has been divided into three clinical subtypes—severe neonatal, mild congenital, and adult-onset—varying in their age at onset, rate of progression, and other associated features. Childhood forms of nemaline myopathy segregate in either an autosomal recessive or an autosomal dominant pattern. Mutations in genes encoding three sarcomeric proteins, including nebulin (*NEB* [MIM 161650]) (Pelin et al. 1999), α-tropomyosin (*TPM3* [MIM 191030]) (Laing et al. 1995; Tan et al. 1999), and α-actin (*ACTA1* [MIM 102610]) (Nowak et al. 1999), have been shown to cause different forms of hereditary NM. Since 1988, we have treated or obtained clinical information on 71 infants and young children from 33 nuclear families with an apparently unique form of NM, which we call Amish nemaline myopathy (ANM), among the Old Order Amish of Lancaster County, Pennsylvania. The purpose of this study was to characterize the genetics of the ANM phenotype and to determine the molecular cause of the disorder.

Received June 5, 2000; accepted for publication August 2, 2000; electronically published August 21, 2000.

Address for correspondence and reprints: Dr. Jennifer J. Johnston, Rm. 3D-45, Bldg. 10, 10 Center Drive, National Institutes of Health, Bethesda, MD 20892-1267. E-mail: jjohnsto@nhgri.nih.gov

0002-9297/2000/6704-0006$02.00

Subjects and Methods

Subjects

We collected information on the mode of presentation, clinical manifestations, affection status of first-degree relatives, age at death, and the genetic relationships of 33 nuclear families having a child affected by ANM in the Old Order Amish genealogy. Four nuclear families with ANM, chosen on the basis of accessibility, underwent phlebotomy and were included in the genotyping for the whole-genome scan. All participants in the latter four families were evaluated clinically by one or more of the authors of the present article, and affection status was ascertained before the study was initiated. Clinical data on children from other families were obtained from clinic reports, through home visits, or by history from the families ascertained by community outreach at the Clinic for Special Children. The study was reviewed and approved by institutional review boards of the National Institutes of Health and Johns Hopkins University.

Pedigree Analysis

Because manual genealogy analysis and pedigree drawing are error prone, we used the Amish Genealogy Database version 2.0 (Agarwala et al. 1999) and the

associated software, PedHunter (Agarwala et al. 1998), to connect the 33 nuclear families with an affected child into "all-shortest-paths" pedigrees. All 33 known families were used for the pedigree analysis, to increase the likelihood of finding the true inheritance path of the mutant allele. We found four all-shortest-paths pedigrees with different founder couples at the top. Each all-shortest-paths pedigree connects the same 65 of 66 obligate carrier parents back to a founder couple, one of whom may have been a carrier. We then formulated a Steiner tree problem to extract a minimal pedigree (also called a "Steiner" pedigree) that has the smallest number of meioses needed to provide one path of inheritance from the founder couple down to each carrier parent (Agarwala et al. 1998). We used the sophisticated branch-and-cut–based Steiner tree software of Koch and Martin (1998) to solve to optimality all four instances corresponding to the different all-shortest-paths pedigrees. From the four possible solutions, we chose the one with the smallest number of individuals. For genetic linkage analyses, the subpedigree of the chosen Steiner pedigree was pruned, removing 29 families and leaving the four sampled nuclear families, their ancestors, and any parent-child links among their ancestors used in the full Steiner pedigree.

Genotyping

Human genomic DNA was isolated from Epstein-Barr virus–immortalized lymphoblastoid lines or fibroblast cell lines, using Puregene DNA isolation kits (Gentra-Systems). Polymorphic microsatellite markers from the ABI PRISM linkage mapping set, version 2, were used for genotyping. Additional markers were identified from genetic maps and were used in fine mapping. These additional markers were ordered as labeled map pairs (Research Genetics) or as custom-labeled oligonucleotides (Life Technologies). For initial homozygosity mapping, three pools of genomic DNA were created, representing parents, unaffected siblings, and affected siblings. All genotyping reactions were performed using the standard protocol from PE Biosystems, with individual reaction components and a reduced reaction volume of 10 μl. PCR products were pooled according to supplied protocols and were loaded on an ABI 377 automated sequencer (filter set D: 5% LongRanger acrylamide gel [FMC Bioproducts]), and the data were analyzed using ABI GeneScan 3.1 and ABI Genotyper 2.1 software (PE Biosystems).

Linkage Analysis

The genetic linkage analyses were performed using the FASTLINK software package, version 4.1P (Lathrop et al. 1984; Cottingham et al. 1993; Schäffer et al. 1994). Loops were broken using the method of Becker et al. (1998). Some multipoint runs were done in parallel (Gupta et al. 1995), using a shared-memory computer and the p4 parallel programming system (Butler and Lusk 1994). In the initial genome scan, we used only four of the five loops (three of the four families) and did two-point analyses on each marker, using equal allele frequencies. For the linkage results shown on chromosome 19, we used all five loops (four families). We used equal allele frequencies in the calculations, because the sample size is sufficiently small and biased toward affected individuals and their parents to preclude reasonable estimates of allele frequencies. In all analyses, we assumed that ANM is a fully penetrant phenotype inherited in an autosomal recessive pattern, with a disease allele frequency of .03. This allele frequency was used to increase the effectiveness of homozygosity mapping, reducing the probability that another allele would be introduced into the pedigree. For comparison purposes, the multipoint linkage was also calculated using an allele frequency of .045 (square root of disease frequency). The Genethon map of the chromosome 19 markers that ultimately proved to be the correct region (numbers in parentheses are the genetic map position [in cM]) is D19S571 (87.7)–D19S572 (93.4)–D19S924 (~94)–D19S927 (94.7)–D19S418 (97.5)–[D19S926, D19S880 (99.6)]–D19S877 (100.1)–D19S210 (105). Analysis with BLAST searches (Altschul et al. 1997) of the sequence-tagged-site content of bacterial artificial chromosomes (BACs), with GenBank accession numbers AC019238 and AC0011476, showed that they both contain D19S418 and D19S926 but not D19S880, supporting the order of markers shown.

Sequence Analysis

The coding exons of *TNNT1,* including the flanking intron sequence, were amplified from genomic DNA from an affected individual, an obligate carrier, and a control. Genomic DNA (50 ng) was amplified in a 50-μl PCR reaction containing 50 pmol each of forward and reverse primer, 1.25 units Ampli*Taq* DNA polymerase (Perkin-Elmer), and 0.2 mM dNTP mix (Pharmacia Biotech). The PCR reaction buffers and annealing temperatures were oligonucleotide-pair specific. Reactions for primer pair 5F/6R contained 10 mM Tris-HCl pH 8.3, 50 mM KCl, and 1.5 mM $MgCl_2$, with an annealing temperature of 67°C. Reactions for 1F/5R, 6F/7R, 7F/9R2, and 11F/14R contained 20 mM Tris-HCl pH 8.4, 50 mM KCl, 1.5 mM $MgSO_4$, and 1 × PCR enhancer (Life Technologies), with an annealing temperature of 60°C; reactions for 9F/11R were run under identical conditions to 1F/5R, except for the addition of 2X PCR enhancer. Initial denaturation for all sets was 3 min at 94°C, followed by 34 cycles of 15 s at 94°C, 15 s at the appropriate annealing temperature, 2 min at 72°C, and a final extension for 7 min at 72°C. Using oligonucleotides

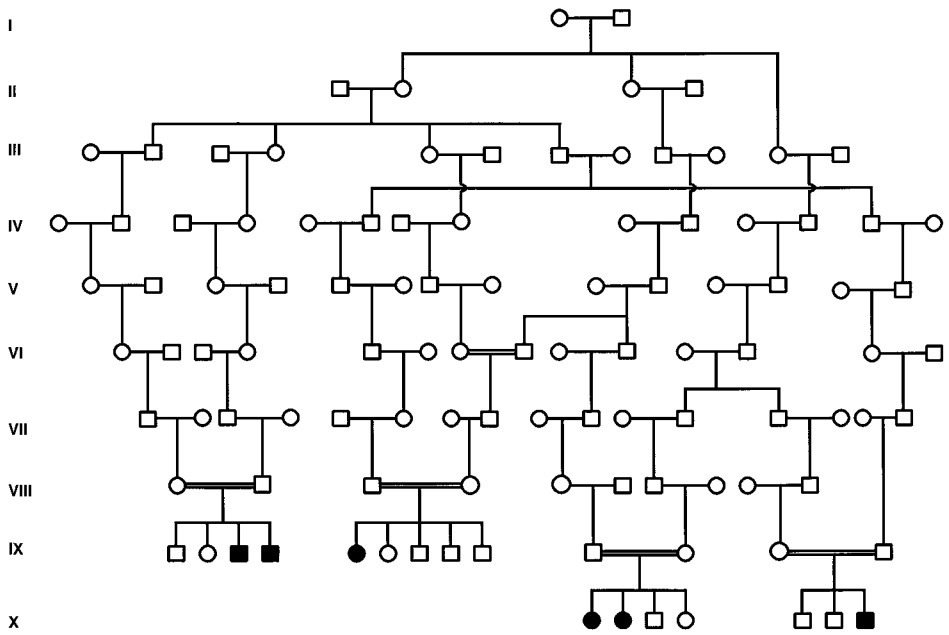

Figure 1 Pedigree used for the whole-genome–scan linkage analysis. The pedigree consisted of four nuclear families, which included six affected patients. These four families are connected in a single subpedigree with five loops. The full pedigree was generated computationally from an Old Order Amish genealogy database and represents a portion of the simplest pedigree that connects 33 affected nuclear families to a putative founder couple who were born in the first half of the 18th century.

10F/11R, exon 11 was amplified from genomic DNA in 136 control individuals and 13 additional family members with ANM. Reactions were run under identical conditions to 1F/5R, except for the absence of PCR enhancer. PCR products were purified and sequenced as described elsewhere (Johnston et al. 1997). Primer sequences named for the *TNNT1* introns from which they are derived are listed in the Appendix.

Results

Phenotype Analysis

All neonates with ANM have tremors that are evident at birth or within a few days of birth and that involve most skeletal muscle groups, especially the muscles of the jaw and lower limbs. These tremors subside over the first 2–3 mo of life. Mild proximal contractures present at birth gradually worsen with age, such that hip abduction is often limited to $\leq 10°$ by age 12 mo. Progressive muscle atrophy and weakness develop simultaneously with the contractures. Gross motor development is limited to rolling side to side, but forearm and hand function is normal, as is apparent intelligence. A characteristic, severe pectus carinatum deformity, with rigidity of the chest wall, develops along with the proximal contractures. The neuromuscular examinations of parents and normally developing siblings are unremarkable. However, several siblings with normal outcomes have had abnormal tremors both in utero and for several weeks after birth. The neurological examinations and, in one case, tests for hypoglycemia and hypocalcemia, were otherwise normal in these siblings. These findings suggest the presence of a subtle carrier effect, but persons with this effect have been considered unaffected, and we have not included samples from any of these individuals in our study.

All routine laboratory chemistries and metabolic studies have been normal in affected patients. Although there often are terminal signs of right-side congestive heart failure, there is no evidence of primary cardiac involvement, and one patient who was studied at age 21 mo

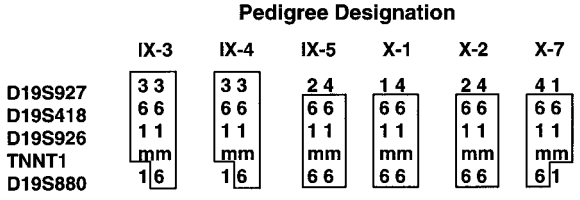

Figure 2 Haplotype analysis of affected persons. To determine the locus boundaries using an analysis of recombinants of affected individuals only, marker D19S927 provides the centromeric boundary and marker D19S880 provides the telomeric boundary. The pedigree designations refer to the generation number in Roman numerals from the pedigree; the individual number is Arabic, numbered from left to right. The allele numbers are the standard CEPH alleles, and "m" signifies the mutant *TNNT1* allele.

Table 1

Two-Point LOD Scores for NM Phenotype and Markers on Chromosome 19

	LOD Score[a] at θ =					
Marker	.0	.01	.03	.05	.07	.1
D19S572	$-\infty$	−.17	.20	.32	.36	.36
D19S924	1.35	1.31	1.21	1.12	1.03	.90
D19S927	$-\infty$	−1.82	−.94	−.57	−.35	−.15
D19S418	2.11	1.98	1.74	1.53	1.33	1.08
D19S926	2.08	1.96	1.72	1.50	1.30	1.05
D19S880	1.96	1.87	1.69	1.53	1.37	1.16
D19S605	.56	.56	.54	.51	.47	.40
D19S877	2.05	1.96	1.77	1.60	1.43	1.21
D19S210	$-\infty$	−.46	−.06	.10	.17	.23

[a] The five-loop version of the pedigree was used for these calculations. Recombination fractions are shown only up to .1, because the markers are very close to each other and we expect the disease gene to be close to these markers.

had a normal electrocardiogram and echocardiogram. Four children in their first year had quadriceps muscle biopsies with both light and electron microscopic examinations. Light microscopy showed prominent type I fiber disproportion, Z-band streaming, and abundant centrally placed refractile rods, as well as areas of myofibrillar disruption and myofiber degeneration (data not shown).

Pedigree and Linkage Analysis

The affected families included 33 nuclear families with one or more children affected with ANM. These families included 33 probands, with a total of 71 affected children and 143 unaffected siblings. The Steiner pedigree used for genetic linkage analysis is shown in figure 1. Prior to performing the full genomewide scan, we used linkage analysis to exclude the gene for *NEB* as a candidate for this disorder (Johnston et al. 1999). In addition, we performed a homozygosity screen using markers from the ABI linkage set surrounding candidate genes for α-tropomyosin and troponin T1, among others. The region on chromosome 19 surrounding the gene for troponin T1 was followed up with additional markers, but the data were not sufficiently convincing (see below). In our analyses of the genome scan data, six regions merited higher resolution genotyping because they had either a marker with a two-point LOD score >1.5 or two adjacent markers with scores >1.0. Of these six regions, only the chromosome 19 region, containing *TNNT1,* had a marker with a two-point LOD score >2.0 and a multipoint LOD score >3.0. We found the two highest-scoring adjacent markers—D19S418 and D19S926—to be the only markers in the study that are homozygous for the same allele in all six genotyped affected individuals. However, both markers are also homozygous for the disease-associated allele in two of the eight obligate carrier parents. Haplotypes of affected individuals are shown in figure 2. Two-point LOD scores are shown in table 1. A three-point LOD score curve using markers D19S418, D19S926, and disease is shown in figure 3; the peak LOD score using a disease allele frequency of .03 is 5.41, and the peak LOD score using a disease allele frequency of .045 is 4.38. These values are consistent (to the third significant digit) throughout the interval D19S418–D19S926. This region of homozygosity was considered inconclusive on the original candidate linkage analysis. In retrospect, that assessment can be attributed to the small region of homozygosity (~2 cM), a double crossover in one nuclear family, and dearth of informative markers in the region. These data strongly support the hypothesis that ANM is inherited in an autosomal recessive pattern and is linked to the chromosome 19 region containing the gene *TNNT1,* suggested by others to be a candidate for NM (Laing 1995).

Mutation Analysis of TNNT1

Because troponin T (TnT) is a sarcomeric protein, we considered *TNNT1* to be a candidate for the ANM disease gene and sequenced the coding region, including the intron/exon borders, in one affected individual, an obligate carrier, and a control. A homozygous nonsense mutation was present in the DNA from the affected individual in exon 11, G579T (Genbank entry S69208), resulting in a stop codon E180X (fig. 4). Although *TNNT1* transcripts undergo alternative splicing of exons 5 and 12, producing up to four isoforms (Samson et al. 1994), exon 11 is present in all known splice products. The change was present in a heterozygous state in the

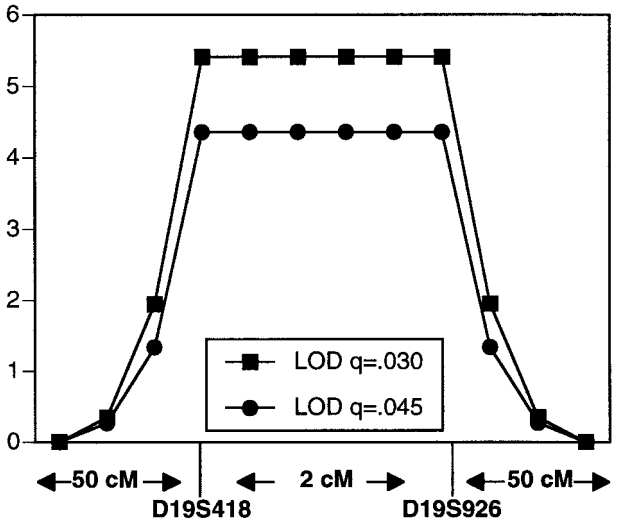

Figure 3 Three-point linkage analysis using two chromosome 19 genetic markers. Calculations were done using disease allele frequencies of .03 and .045.

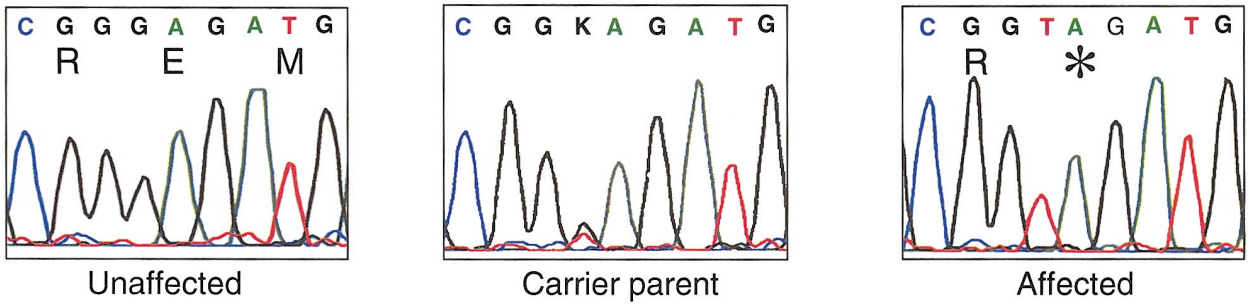

Figure 4 Sequence traces of exon 11 of the *TNNT1* gene in an unaffected control, a carrier parent, and an affected patient. The carrier is heterozygous for the G579T substitution, and the affected individual is homozygous for this change. The nucleotide and predicted amino acid sequence is shown above the traces, with the stop codon labeled by an asterisk (*).

obligate carrier and absent from the control sample. All 15 available samples from the full pedigree were analyzed by sequencing, and the mutation was found to segregate with the disease state. The mutation was not found in 200 non-Amish control chromosomes nor in 72 chromosomes from Amish individuals drawn from nuclear families unaffected by ANM. Because genetic control samples must be acquired from unrelated individuals, it is impossible to gather true Amish controls, since all Amish persons are related.

Discussion

ANM is a distinct form of NM that segregates in an autosomal recessive pattern. With the identification of a mutation in *TNNT1* (gene encoding slow skeletal muscle TnT), it becomes the fourth form of NM to be associated with an abnormality of a protein component of the thin filament of the sarcomere. Nemaline bodies, the hallmark of NM, are histochemically and ultrastructurally similar to the Z disk of the sarcomere and are often found in physical continuity with the Z disk in NM. It is notable, therefore, that all four of the genes associated with NM code for protein components integral to the thin filament rather than protein components found solely in the Z disk. However, one of the gene products responsible for NM—nebulin—is thought to be an important regulator of the assembly and organization of the Z disk (Pelin et al. 1999). The other three gene products associated with NM—α-actin (Nowak et al. 1999), α-tropomyosin (Laing et al. 1995; Tan et al. 1999) and, with this article, slow skeletal TnT—interact with one another and ultimately regulate the development of muscle contraction. Like the more heterogeneous adult forms of NM, the proliferation of nemaline bodies in each of these latter three disorders may be a secondary consequence of abnormal regulation of force within the sarcomere (North et al. 1997; Michele et al. 1999).

The mapping of this phenotype was facilitated by the structure of the Amish population. The Old Order Amish are a genetic isolate with a high rate of consanguinity and multiple disorders with proved or apparent founder effects. The Old Order Amish trace their ancestry to 50–100 European immigrants of the mid to late 1700s. In the Amish Genealogy Database, version 2.0, the average inbreeding coefficient is .0187 (Agarwala et al. 1999). The genetic origins of this population and their strict endogamy predispose them to manifest rare disorders that are inherited in an autosomal recessive pattern. These same genetic and demographic features of the Old Order Amish advance the identification of rare disease-causing genes that are found within this group. The technique of whole-genome linkage analysis via identification of regions of homozygosity among affected individuals is particularly suited to this population (McKusick 2000) and was a productive approach in this instance to map, clone, and identify a nonsense mutation in *TNNT1*, coding for slow skeletal TnT as the cause of AMN.

The identified mutation of *TNNT1* predicts a truncation of the TnT protein at amino acid 180, removing the C-terminal 83 amino acids that include the principal site of interaction with the other two components of the troponin complex, troponin I (TnI) and troponin C (TnC). In addition, a second site of interaction with tropomyosin, which is dependent on Ca^{++} concentration, is also in the deleted part of the protein. The remaining N-terminal portion of TnT forms the whole of the troponin tail region, which anchors the complex to tropomyosin. A schematic diagram of these interactions is shown in figure 5 (Cohen 1975; Flicker et al. 1982). There are at least three potential consequences of this mutation: the mutant message may be subject to accel-

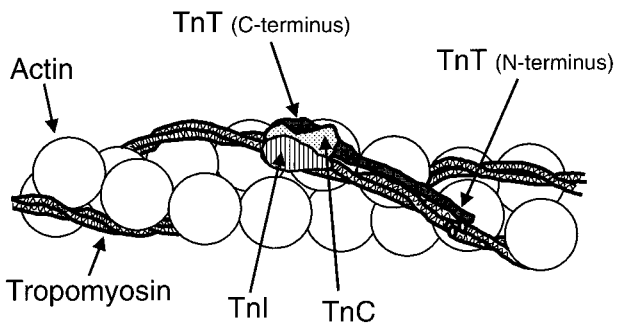

Figure 5 Thin filament structure showing troponin complex, tropomyosin, and actin. TnC, TnI, and the C-terminal portion of TnT bind near Cys190 of tropomyosin. The N-terminal portion of TnT extends along the C-terminal half of tropomyosin. The predicted truncation in ANM would delete a part of the C-terminal end of the TnT molecule that interacts with TnI, TnC, and tropomyosin.

erated nonsense-mediated decay (Maquat 1995), the protein may be unstable or improperly localized, or the truncated protein may be translated in normal abundance and appropriately bound to tropomyosin in the thin filament but deficient in the ability to interact properly with TnI and TnC. We speculate that the recessive inheritance pattern in ANM may be indicative of accelerated nonsense-mediated decay or protein instability, compared with the dominant inheritance pattern seen in the family with NM segregating a missense mutation in TPM3 (Laing et al. 1995) and the families segregating missense mutations for ACTA1 (Nowak et al. 1999). Production of aberrant sarcomeric proteins may be less well tolerated than haploinsufficiency of these same proteins.

In any of these cases, this abnormality of TnT is likely to disturb the coupling of excitation to contraction within muscle fibers. At rest, and with low concentrations of Ca^{++}, TnI interacts with α-actin and α-tropomyosin to block the ATPase of actomyosin and thus inhibit contraction. With muscle fiber depolarization, Ca^{++} released from the sarcoplasmic reticulum is bound to TnC, and in the presence of TnT, a conformational change of the complex releases the inhibitory effect of TnI upon actomyosin.

Hypertrophic cardiomyopathy (HCM), like NM, has been associated with mutations of protein components of the thin filament of the sarcomere, including cardiac TnT (Laing 1995). A variety of deletion, splice site, and missense mutations in the gene for cardiac TnT (*TNNT2*) cause familial HCM (Perry 1998). A splice-site mutation in intron 16 of *TNNT2,* seen in one individual with familial HCM, is predicted to lead to production of a truncated protein. Transfection of this mutation into a quail myotube expression system resulted in disorganized myofibrils and a greatly diminished Ca^{++}-activated force of contraction (Watkins et al. 1996; Perry 1998), indicating that expression of a truncated cardiac TnT may have a dominant negative effect on muscle. We hypothesize that mutations in *TNNT1* manifest in an autosomal recessive pattern, whereas *TNNT2* mutations segregate in an autosomal dominant pattern, because skeletal and cardiac muscle may have different phenotypic thresholds.

It is interesting to note that mutations in the *Caenorhabditis elegans* TnT (*mup-2*) gene lead to myocyte dysfunction suggestive of the phenotype seen in ANM. The recessive inheritance pattern of human *TNNT1* mutations is consistent with that seen in the *C. elegans* mutants (both truncation and null mutants). Worms homozygous for either a null allele or an amino terminal truncation mutation of *mup-2* show a phenotype with apparent hypercontraction and ultimate detachment of body wall muscles (Myers et al. 1996). Prior to detachment, the embryos show uncoordinated, slow twitching, rather than the vigorous rolling typical of wild-type embryos. Mutations affecting voltage-dependent muscle Ca^{++} release, TnC, or sarcomere assembly are epistatic to *mup-2,* which suggests that the *mup-2* phenotype is not due to sustained Ca^{++}-independent contraction but is caused by aberrant regulation of contraction (McArdle et al. 1998).

In vitro studies of human fast skeletal TnT show that truncated TnT protein does not bind TnI/TnC as efficiently as wild-type TnT (Jha et al. 1996). The authors propose that, in the absence of TnT tethering TnI/TnC to tropomyosin, inhibition of contraction is not established normally after contraction, leading to the phenotypic twitching and ultimate muscle detachment. Although we have treated ANM patients with myotonia-limiting drugs, such as carbamazepine and mexilitene, in an attempt to limit the progression of the chest deformity and associated respiratory insufficiency, such treatments have had minimal benefit. Further understanding of the cellular pathogenesis of ANM and study of the identified mutation in potential animal models should stimulate research into effective treatments for this relentlessly progressive disorder.

Acknowledgments

We wish to thank Ralph Kuncl for identification of nemaline myopathy in biopsy specimens. We would also like to thank Joie Davis for her contribution to the fieldwork.

Appendix

Primer	Sequences
1F	TCCCTAAGACCCAGGAATCCG
4F	CGGTCCTCTAACAGCCTCTCACG
5R2	GGCTTAAAGGACCGGGCCTGG
5F	TGACCCTCTTCCTCCTTTACAGC
6R	TCTGCCTTTCTCACACCTTGTCTC
6F	CTACCTCACTGGACGGCACATC
7R	GCCTCGTGTTTGACACTAATCAGC
7F	GCTGATTAGTGTCAAACACGAGGC
9R2	GGCATCCGGCTGAAGAAGTAAC
9F	TGCGTTTCTGCTGGTTCTGATG
10R	CTCAGCCCCTCCTCCGTTAGG
10F	CTGTGGTCCCAACATGGAAATGG
11R	CCTTTATCCCCCTGTCTCACACC
11F	TGAACAAAATGGTGCCGACAAC
13R	ACCCAGGATTCCGAGAGCAGAG
13F	TGCTTCCTTTGGGCAGGGAG
14R	ACATCCAGGAGGGGAACTGC

Electronic-Database Information

Accession numbers and URLs for data in this article are as follows:

GenBank, http://www.ncbi.nlm.nih.gov/Genbank/index.html (for BAC clones AC019238 and AC0011476 and for *TNNT1* sequence S69208)

Généthon, ftp://ftp.genethon.fr/pub/Gmap/Nature-1995/data/data_chrom19 (for microsatellite markers from the chromosome 19 region)

Online Mendelian Inheritance in Man (OMIM), http://www.ncbi.nlm.nih.gov/Omim/ (for NM [MIM 256030, 161800], *NEB* [MIM 161650], *TPM3* [MIM 191030], and *ACTA1* [MIM 102610])

References

Agarwala R, Biesecker LG, Hopkins KA, Francomano CA, Schäffer AA (1998) Software for constructing and verifying pedigrees within large genealogies and an application to the Old Order Amish of Lancaster County. Genome Res 8:211–221

Agarwala R, Biesecker LG, Tomlin JF, Schäffer AA (1999) Towards a complete North American Anabaptist genealogy: a systematic approach to merging partially overlapping genealogy resources. Am J Med Genet 86:156–161

Altschul SF, Madden TL, Schäffer AA, Zhang J, Zhang Z, Miller W, Lipman DJ (1997) Gapped BLAST and PSI-BLAST: a new generation of protein database search programs. Nucleic Acids Res 25:3389–3402

Becker A, Geiger D, Schäffer AA (1998) Automatic selection of loop breakers for genetic linkage analysis. Hum Hered 48:49–60

Butler R, Lusk E (1994) The p4 parallel programming system. Parallel Computing 20:547–564

Cohen C (1975) The protein switch of muscle contraction. Sci Am 233:36–45

Cottingham RW Jr, Idury RM, Schäffer AA (1993) Faster sequential genetic linkage computations. Am J Hum Genet 53: 252–263

Flicker PF, Phillips GN Jr, Cohen C (1982) Troponin and its interactions with tropomyosin: an electron microscope study. J Mol Biol 162:495–501

Gupta SK, Schäffer AA, Cox AL, Dwarkadas S, Zwaenepoel W (1995) Integrating parallelization strategies for linkage analysis. Comput Biomed Res 28:116–139

Jha PK, Leavis PC, Sarkar S (1996) Interaction of deletion mutants of troponins I and T: COOH-terminal truncation of troponin T abolishes troponin I binding and reduces Ca2+ sensitivity of the reconstituted regulatory system. Biochemistry 35:16573–16580

Johnston J, Kelley RI, Feigenbaum A, Cox GF, Iyer GS, Funanage VL, Proujansky R (1997) Mutation characterization and genotype-phenotype correlation in Barth syndrome. Am J Hum Genet 61:1053–1058

Johnston JJ, Kelley RI, Morton DH, Crawford TO, Biesecker LG, Francomano CA (1999) Haplotype analysis of markers on chromosome 2q21.2-q22 in nemaline myopathy in the Amish: Evidence for genetic heterogeneity. Am J Hum Genet 65:A256

Koch T, Martin A (1998) Solving Steiner tree problems in graphs to optimality. Networks 32:207–232

Laing NG (1995) Inherited disorders of contractile proteins in skeletal and cardiac muscle. Curr Opin Neurol 8:391–396

Laing NG, Wilton SD, Akkari PA, Dorosz S, Boundy K, Kneebone C, Blumbergs P, White S, Watkins H, Love DR, et al (1995) A mutation in the a-tropomyosin gene TPM3 associated with autosomal dominant nemaline myopathy. Nat Genet 9:75–79

Lathrop GM, Lalouel J-M, Julier C, Ott J (1984) Strategies for multilocus linkage analysis in humans. Proc Natl Acad Sci USA 81:3443–3446

Maquat L (1995) When cells stop making sense: effects of nonsense codons on RNA metabolism in vertebrate cells. RNA 1:453–465

McArdle K, Allen TS, Bucher EA (1998) Ca2+-dependent muscle dysfunction caused by mutation of the *Caenorhabditis elegans* troponin T-1 gene. J Cell Biol 143:1201–1213

McKusick VA (2000) Ellis-van Creveld syndrome and the Amish. Nat Genet 24:203–204

Michele DE, Albayya FP, Metzger JM (1999) A nemaline myopathy mutation in alpha-tropomyosin causes defective regulation of striated muscle force production. J Clin Invest 104:1575–1581

Myers CD, Goh PY, Allen TS, Bucher EA, Bogaert T (1996) Developmental genetic analysis of troponin T mutations in striated and nonstriated muscle cells of *Caenorhabditis elegans*. J Cell Biol 132:1061–1077

North KN, Laing NG, Wallgren-Pettersson C, The ENMC International Consortium on Nemaline Myopathy (1997) Nemaline myopathy: current concepts. J Med Genet 34: 705–713

Nowak KJ, Wattanasirichaigoon D, Goebel HH, Wilce M, Pelin K, Donner K, Jacob RL, Hubner C, Oexle K, Anderson JR, Verity CM, North KN, Iannaccone ST, Muller CR,

Nurnberg P, Muntoni F, Sewry C, Hughes I, Sutphen R, Lacson AG, Swoboda KJ, Vigneron J, Wallgren-Pettersson C, Beggs AH, Laing NG (1999) Mutations in the skeletal muscle alpha-actin gene in patients with actin myopathy and nemaline myopathy. Nat Genet 23:208–212

Pelin K, Hilpelä P, Donner K, Sewry C, Akkari PA, Wilton SD, Wattanasirichaigoon D, Bang ML, Centner T, Hanefeld F, Odent S, Fardeau M, Urtizberea JA, Muntoni F, Dubowitz V, Beggs AH, Laing NG, Labeit S, de la Chapelle A, Wallgren-Pettersson C (1999) Mutations in the nebulin gene associated with autosomal recessive nemaline myopathy. Proc Natl Acad Sci USA 96:2305–2310

Perry SV (1998) Troponin T: genetics, properties and function. J Muscle Res Cell Motil 19:575–602

Samson F, Mesnard L, Mihovilovic M, Potter TG, Mercadier JJ, Roses AD, Gilbert JR (1994) A new human slow skeletal troponin T (TnTs) mRNA isoform derived from alternative splicing of a single gene. Biochem Biophys Res Commun 199:841–847

Schäffer AA, Gupta SK, Shriram K, Cottingham RW Jr (1994) Avoiding recomputation in linkage analysis. Hum Hered 44: 225–237

Tan P, Briner J, Boltshauser E, Davis MR, Wilton SD, North K, Wallgren-Pettersson C, Laing NG (1999) Homozygosity for a nonsense mutation in the α-tropomyosin slow gene TPM3 in a patient with severe infantile nemaline myopathy. Neuromuscul Disord 9:573–579

Watkins H, Seidman CE, Seidman JG, Feng HS, Sweeney HL (1996) Expression and functional assessment of a truncated cardiac troponin T that causes hypertrophic cardiomyopathy: evidence for a dominant negative action. J Clin Invest 98:2456–2461